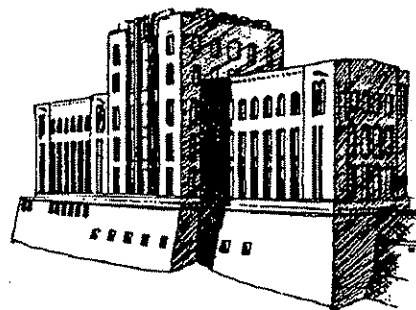


FIELD MEASUREMENTS OF ICE SCRAPING LOADS ON FRONT MOUNTED PLOW BLADES

**Final Report
of
Project HR 374
Iowa Department of Transportation
and
Iowa Highway Research Board**

by

Wilfrid A. Nixon, Yingchang Wei, and Andrew E. Whelan



IIHR Technical Report No. 388

Iowa Institute of Hydraulic Research
College of Engineering
The University of Iowa
Iowa City IA 52242-1585

October 1997

ACKNOWLEDGEMENTS

This project was possible by funding from the Iowa Department of Transportation and the Iowa Highway Research Board, Project Number HR 374. This support is greatly acknowledged.

The support of the Director of the Iowa Institute of Hydraulic Research, Dr. V.C. Patel, enable this study to proceed. The shop staff at IIHR, led by Mr. Jim Goss, made these experiments possible with their assistance. A special thanks goes to Mr. Doug Houser and Mr. Mark Wilson. The assistance of Ms. Zhongwei Shi in preparing the final report is greatly acknowledged.

The truck used in this testing was provided by the Iowa Department of Transportation. The assistance of Mr. Lee Smithson throughout the project is greatly appreciated. Permission to use the test site at Coralville Reservoir was given by the US Army Corps of Engineers.

ABSTRACT

Removal of ice from roads is of the more challenging tasks in winter highway maintenance. The best mechanical method is to use a truck with underbody plow blade, but such equipment is not available to all agencies charged with winter maintenance operations. While counties and cities often use motor graders to scrape ice, it would be of great benefit if front mounted plows could be used effectively for ice removal. To reveal and understand the factors that influence the performance of these plows, measurement of the forces experienced by the plow blades during ice scraping is desirable.

This study explores the possibility of using accelerometers to determine the forces on a front-mounted plow when scraping ice. The plow was modeled by using a dynamic approach. The forces on the plow were to be determined by the measurement of the accelerations of the plow. Field tests were conducted using an "as is" front-mounted plow instrumented with accelerometers. The results of the field tests indicate that in terms of ice removal, the front-mounted plow is not favorable equipment. The major problem in this study is that the front mounted plow was not able to cut ice, and therefore experienced no significant scraping forces. However, the use of accelerometers seems to be promising for analyzing the vibration problems of the front-mounted plow.

LIST OF FIGURES

Figure 1.	The truck and the front-mounted plow used for field tests.....	3
Figure 2.	The schematic of the truck and the front-mounted plow.....	4
Figure 3.	The separated plow showing the acting forces.....	5
Figure 4.	The separated carrier showing the acting forces.....	6
Figure 5.	The relative position between the plow and the carrier in their motion.....	8
Figure 6.	Determination of the accelerations of the plow by three accelerometers.....	10
Figure 7.	The placement of the accelerometers for the truck, carrier, and plow.....	11
Figure 8.	Accelerometers installed in the boxes attached to the plow and carrier.....	12
Figure. 9	Details of the accelerometers inside the boxes.....	13
Figure. 10	(a) The power/coupler for the accelerometers.....	14
	(b) The computer with data acquisition system.....	15
Figure. 11	(a) The acceleration in x-direction measured by accelerometer A.....	19
	(b) The acceleration in y-direction measured by accelerometer B.....	20
	(c) The acceleration in x-direction measured by accelerometer C.....	21
	(d) The acceleration in y-direction measured by accelerometer D.....	22
	(e) The acceleration in x-direction measured by accelerometer E.....	23
	(f) The acceleration in y-direction measured by accelerometer F.....	24
	(g) The acceleration in x-direction measured by accelerometer G.....	25
	(h) The acceleration in y-direction measured by accelerometer H.....	26
Figure. 12	(a) The power spectrum of the signal from accelerometer A.....	27
	(b) The power spectrum of the signal from accelerometer B.....	28
	(c) The power spectrum of the signal from accelerometer C.....	29
	(d) The power spectrum of the signal from accelerometer D.....	30
	(e) The power spectrum of the signal from accelerometer E.....	31
	(f) The power spectrum of the signal from accelerometer F.....	32
	(g) The power spectrum of the signal from accelerometer G.....	33
	(h) The power spectrum of the signal from accelerometer H.....	34

FIELD MEASUREMENTS OF ICE SCRAPING LOADS ON FRONT MOUNTED PLOW BLADES

I. INTRODUCTION

Winter weather can pose a variety of hazards to the traveling public. In the Midwestern U.S., one of the more serious hazards is freezing rain. Under extreme circumstances, a freezing rain event may leave up to 25mm (about 1 inch) or more ice on the road surface. This makes the road surface extremely slick, and makes safe driving almost impossible.

Removing such ice from the road is of the more challenging tasks in Winter Highway Maintenance. The best mechanical method is to use a truck with an underbody plow blade, but such equipment is not available to all agencies charged with Winter Maintenance Operations. While counties and cities often use motor graders to scrape ice under such conditions, it would be of great benefit if front mounted plows could be used effectively to scrape ice.

While front mounted plows are not ideal for ice removal, in large part because they cannot be forced down into the ice in the same way as an underbody plow can, it is still important to try to get the best possible performance from such plows, especially since they may be the only type of equipment available. Questions arise as to whether a heavy or light plow is best suited for these tasks, whether these plows can be set to a certain angle to optimize the ice removal process, and whether the performance of these plows might be improved by using an appropriate type of cutting edge. Furthermore, to reveal and understand the factors that influence the performance of front mounted plows, measurement of the forces experienced by the plow blades during ice scraping is desirable.

This study builds off the expertise developed in the project HR 334, in which a truck with an underbody plow blade was instrumented and the forces required to scrape ice with the equipment were measured (Nixon and Frisbie, 1993). For an underbody plow the cutting edge is pushed into the ice deliberately and the forces experienced by the

cutting edge are fairly stable. This allows the forces on the cutting edge to be measured by using pressure gages in the hydraulic lines to the cylinders responsible for the download force and the rotation of the blade. For a front plow, however, the blade is kept in contact with the surface of ice by its own weight, which creates a much more dynamic situation. The use of pressure gages would not pick up the dynamic responses of the blade. To measure the forces on the front mounted plow blade, it is necessary to develop an appropriate methodology to deal with the dynamic situation of the plow.

The aim of this study is to conduct field measurements of ice scraping loads on front mounted plow blades and to indicate under what conditions the optimal performance of such plows can be achieved.

II. INSTRUMENTATION AND MODELING

One key aspect of this study is to instrument a front mounted plow so that the forces experienced by the plow during the scraping of ice and compacted snow can be measured. Since the operation of front mounted plow brings about much more dynamic problems than an underbody plow, it is necessary to measure the accelerations of the plow. These accelerations can then be used to calculate the forces acting on the plow. To calculate these forces, two things are necessary. First, the accelerations of the plow have to be measured using accelerometers, and second, the plow assembly has to be modeled in such a way that the forces that cause the accelerations can also be modeled.

A. Selection of Accelerometers. Based on the experience gained from project HR334 (Nixon and Frisbie, 1993), it was decided to use Kistler piezo accelerometers with measurement range from -50g to +50g ($g=9.8\text{m/s}^2$) which would allow a front plow to reach a maximum acceleration of 490m/s^2 . This proved be sufficient to account for any dynamic responses of the front plow.

B. Plow Modeling. The truck (1982 Ford) and the front mounted plow used for this study were provided by the Iowa Department of Transportation (IDOT) and are

shown in Fig. 1. The plow is connected to the truck by a carrier. The connection from plow to carrier and from carrier to truck can be considered hinge joints. This can be simplified as the mechanical system schemed in Fig. 2. As shown in Fig. 2, the system consists of three parts: the truck, the carrier, and the plow. In addition to the hinge joint between the plow and the carrier, a spring connecting these two parts was installed to keep the plow in place while allowing it to rotate when hitting irregular spots such as protruding concrete joint and manhole covers. When scraping ice or snow the motion of the plow consists of translation and rotation. To find out the forces resulting in the accelerations of the plow we separate the plow from the system, as presented in Fig. 3. The following equations (**Plow Equations**) are readily derived from Fig. 3:



Figure 1. The truck and the front-mounted plow used for field tests

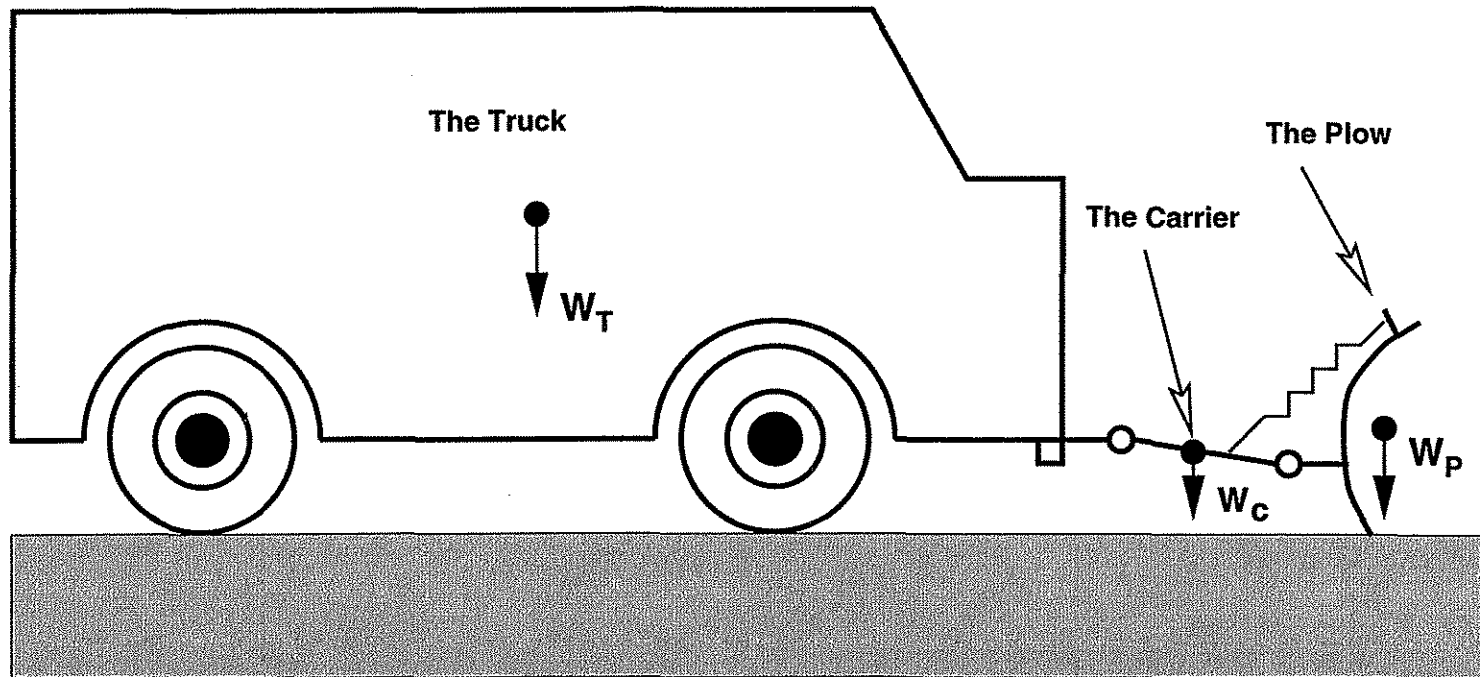


Figure 2 The schematic of the truck and the front mounted plow. Each centroid of the system has an accelerometer package to measure the linear and rotation accelerations.

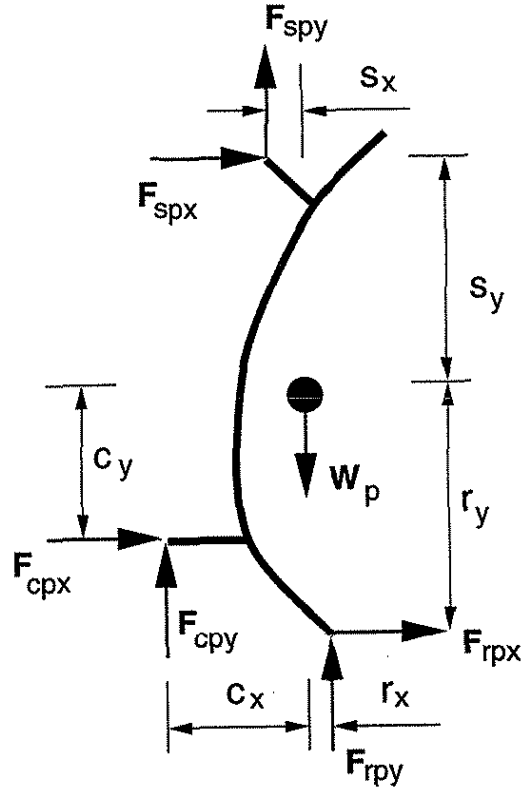


Figure 3. The separated plow showing the acting forces

$$\sum F_x = F_{cpx} + F_{rpx} + F_{spx} = m_p a_{px} \quad (1)$$

$$\sum F_y = F_{cpy} + F_{rpy} + F_{spx} = m_p a_{py} + W_p \quad (2)$$

$$\sum M_c = F_{cpx} c_y + F_{rpx} r_y - F_{spx} s_x - F_{cpy} c_x + F_{rpy} r_x - F_{spx} s_y = I_{pc} \phi_p \quad (3)$$

where F_{cpx} : the acting force of carrier on the plow in the x-direction,

F_{rpx} : the resistant force on the plow in the x-direction,

F_{spx} : the acting force of spring on the plow in the x-direction,

F_{cpy} : the acting force of carrier on the plow in the y-direction,

F_{rpy} : the resistant force on the plow in the y-direction,

F_{spx} : the acting force of spring on the plow in the y-direction,

a_{px} : the linear acceleration of the plow in the x-direction,

a_{py} : the linear acceleration of the plow in the y-direction,

φ_p : the rotation acceleration of the plow,

I_{pc} : the moment of inertia of the plow,

m_p : the mass of the plow, and

W_p : the weight of the plow.

Similarly, the forces acting on the carrier can be found out from the separated diagram in Fig.4, and the **Carrier Equations** are obtained as following.

$$F_x = F_{pcx} + F_{tcx} + F_{scx} = m_c a_{cx} \quad (4)$$

$$F_y = F_{pcy} + F_{tcy} + F_{scy} = m_c a_{cy} + W_c \quad (5)$$

$$M_c = F_{pcx}u_y - F_{tcx}h_y + F_{scx}e_y + F_{pcy}u_x - F_{tcy}h_x + F_{scy}e_x = I_{cc} \varphi_c \quad (6)$$

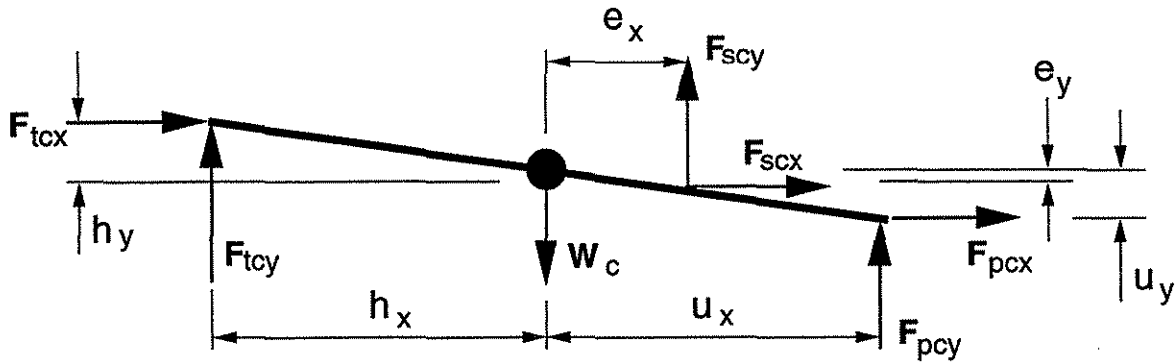


Figure 4. The separated carrier showing the acting forces

where F_{pcx} : the acting force of plow on the carrier in the x-direction,

F_{tcx} : the acting force of truck on the carrier in the x-direction,

F_{scx} : the acting force of spring on the carrier in the x-direction,

F_{pcy} : the acting force of plow on the carrier in the y-direction,

F_{tcy} : the acting force of truck on the carrier in the y-direction,

F_{scy} : the acting force of spring on the carrier in the y-direction,

a_{cx} : the linear acceleration of the carrier in the x-direction,

- \mathbf{a}_{cy} : the linear acceleration of the carrier in the y-direction,
- φ_c : the rotation acceleration of the carrier,
- I_{cc} : the moment of inertia of the carrier,
- m_c : the mass of the carrier, and
- W_c : the weight of the carrier.

In the above six equations, the accelerations (\mathbf{a}_{px} , \mathbf{a}_{py} , \mathbf{a}_{cx} , \mathbf{a}_{cy} , φ_p , and φ_c) are to be obtained by the accelerometers (to be discussed further in the following section). The masses and the centroids of the carrier and plow as well as the distances between the centroids and the acting forces (see Fig. 3 and 4) can be measured. The unknowns in the equations are the forces. However, the spring force \mathbf{F}_s (resultant of \mathbf{F}_{spx} and \mathbf{F}_{spx} or \mathbf{F}_{scy} and \mathbf{F}_{scy}) can be determined by the procedures described below.

Since the accelerations of the plow \mathbf{a}_{px} , \mathbf{a}_{py} , and φ_p are known, and the initial conditions are also known (the truck begins to accelerate from a stationary position), the displacements and rotation of the plow centroid \mathbf{x}_p , \mathbf{y}_p , and ω_p can be found by integrating \mathbf{a}_{px} , \mathbf{a}_{py} , and φ_p twice, respectively. Similarly, the displacements and rotation of the carrier centroid \mathbf{x}_c , \mathbf{y}_c , and ω_c can be determined using the measured \mathbf{a}_{cx} , \mathbf{a}_{cy} , and φ_c . These allow the length l of the spring connecting the plow and the carrier to be calculated as following.

Refer to Fig. 5 and let

$$A = \begin{bmatrix} \cos \alpha & -\sin \alpha \\ \sin \alpha & \cos \alpha \end{bmatrix} \quad B = \begin{bmatrix} \cos \beta & -\sin \beta \\ \sin \beta & \cos \beta \end{bmatrix}$$

where $\alpha = \omega_c$, and $\beta = \omega_p$, we have the spring length

$$l = \left\| \vec{a} + A\vec{d} - \vec{b} - B\vec{c} \right\|.$$

Knowing the spring length change, the spring force (\mathbf{F}_s) is readily obtained by

$$\mathbf{F}_s = K(l)l$$

where $K(l)$ is the spring modulus which can be determined experimentally.

Given that the spring forces are now known and the forces across the plow carrier connection are equal, i.e.

$$F_{cpx} = -F_{pcx} \quad (7)$$

$$F_{cpy} = -F_{pcy} \quad (8)$$

we therefore have 8 independent equations (equations (1), (2), (3) in Plow Equations, equations (4), (5), (6) in Carrier Equations, and equations (7) and (8)) to solve for 8 unknown forces, namely F_{cpx} , F_{cpy} , F_{ipx} , F_{ipy} , F_{pcx} , F_{pcy} , F_{icx} , and F_{icy} . In particular, F_{ipx} and F_{ipy} are the forces that the cutting edge experiences when scraping ice.

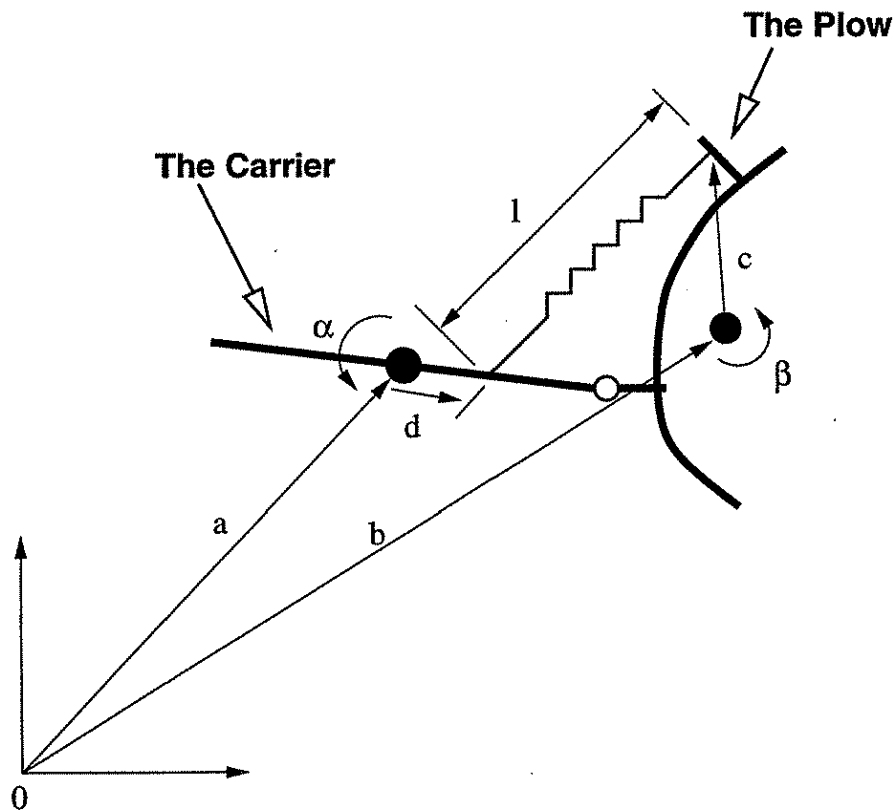


Figure 5. The relative position between the plow and the carrier in their motion

The above discussion demonstrates that it is possible to determine the forces on a front mounted plow through the measurement of accelerations of the plow and the carrier. This approach not only can measure the forces on the cutting edge, but also can reveal the interaction between the plow and the carrier as well as the carrier and the truck. However, experience has shown that deriving the spring force from the accelerations is less preferable than a direct measure of this spring force. The double integration can give rise to rapid propagation of errors under certain circumstances.

C. Instrumentation. As mentioned above, the acceleration parameters in the Plow and Carrier Equations are to be determined by the accelerometers. To accomplish this task, it is necessary to decide how many accelerometers are needed and how they should be installed. In the case of the plow for example, the accelerations of the plow are depicted by \mathbf{a}_{px} , \mathbf{a}_{py} , and φ_p . To determine these three parameters, we need three accelerometers to be installed on the plow in such a way that the accelerometers are coplanar with the centroid of the plow, as illustrated in Fig. 6. The accelerometer 1 in Fig. 6 is installed to measure the x-component of the acceleration (\mathbf{a}_{1x}) at that point, and the accelerometers 2 and 3 are used to measure the y-components of the accelerations (\mathbf{a}_{2y} and \mathbf{a}_{3y}) at the other two points.

The measured acceleration \mathbf{a}_{1x} consists of two parts: one is caused by displacement of the plow and is represented by \mathbf{a}_{px} , the other is caused by rotation of the plow and is represented by \mathbf{a}_{rx} , i.e., $\mathbf{a}_{1x} = \mathbf{a}_{px} + \mathbf{a}_{rx}$. From Fig. 6,

$$\mathbf{a}_{rx} = \mathbf{a}_r \cos[\alpha_1 - \arctan(a_t/a_n)],$$

where $\mathbf{a}_r = (\mathbf{a}_t^2 + \mathbf{a}_n^2)^{1/2}$, $\mathbf{a}_t = \varphi_p r_1$, and $\mathbf{a}_n = \omega_p^2 r_1$, here ω_p is the angular velocity which can be determined by the integration of φ_p . Applying the same analysis for \mathbf{a}_{2y} and \mathbf{a}_{3y} , we therefore have

$$\mathbf{a}_{1x} = \mathbf{a}_{px} + r_1 [(\varphi_p)^2 + (\omega_p^2)^2]^{1/2} \cos[\alpha_1 - \arctan(\omega_p^2/\varphi_p)]$$

$$\mathbf{a}_{2y} = \mathbf{a}_{py} + r_2 [(\varphi_p)^2 + (\omega_p^2)^2]^{1/2} \sin[\alpha_2 - \arctan(\omega_p^2/\varphi_p)]$$

$$\mathbf{a}_{3y} = \mathbf{a}_{py} + r_3 [(\varphi_p)^2 + (\omega_p^2)^2]^{1/2} \sin[\alpha_3 - \arctan(\omega_p^2/\varphi_p)]$$

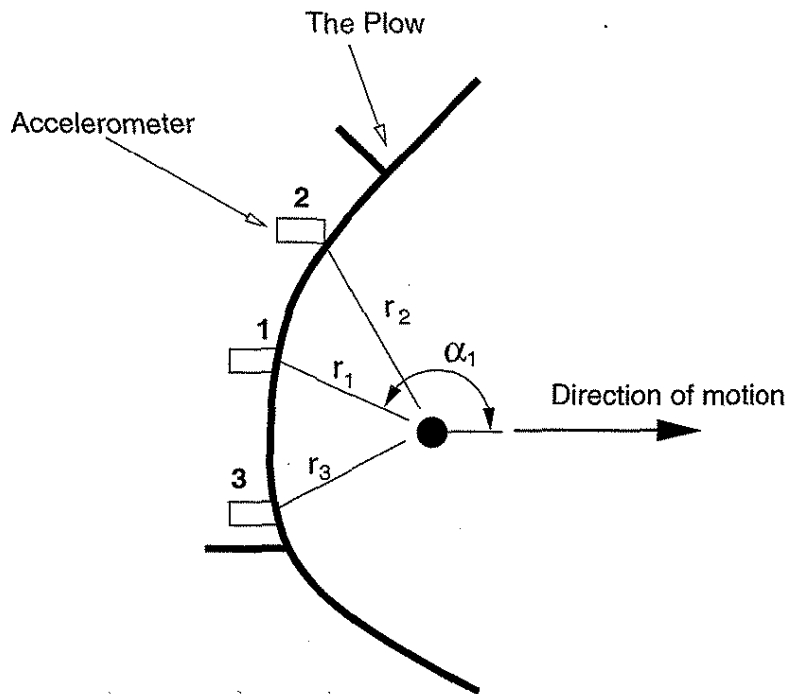


Figure 6. Determination of the accelerations of the plow by three accelerometers

where r_1 , r_2 , and r_3 are the distances between the accelerometers and the centroid of the plow, and α_1 , α_2 , and α_3 are angles that r_1 , r_2 , and r_3 make with the motion direction (i.e. the horizontal direction) of the plow. These three equations allow a_{px} , a_{py} , and φ_p to be found out uniquely. Applying the same approach to the carrier, the accelerations of the carrier, a_{cx} , a_{cy} , and φ_c , can be determined by using three accelerometers with similar configuration. Thus, six accelerometers are needed in order to determine 6 acceleration parameters in the Plow and Carrier Equations. In this study, however, it was believed that the information of the dynamic response of the truck itself might be useful. Therefore, 4 additional accelerometers were mounted on the truck frame, with three of them used to measure the accelerations of the truck and one used to pick up the lateral motion signals. In addition, two additional accelerometers were placed at both ends of the plow to check if the plow (cutting edge) experiences a lateral rotation. Thus a total of 12 accelerometers

were used in this study. It is noted, however, that for the purpose of determination of the forces on a front mounted plow as shown in Fig. 3, only six accelerometers are strictly necessary.

The placement of the accelerometers is schemed in Fig. 7.

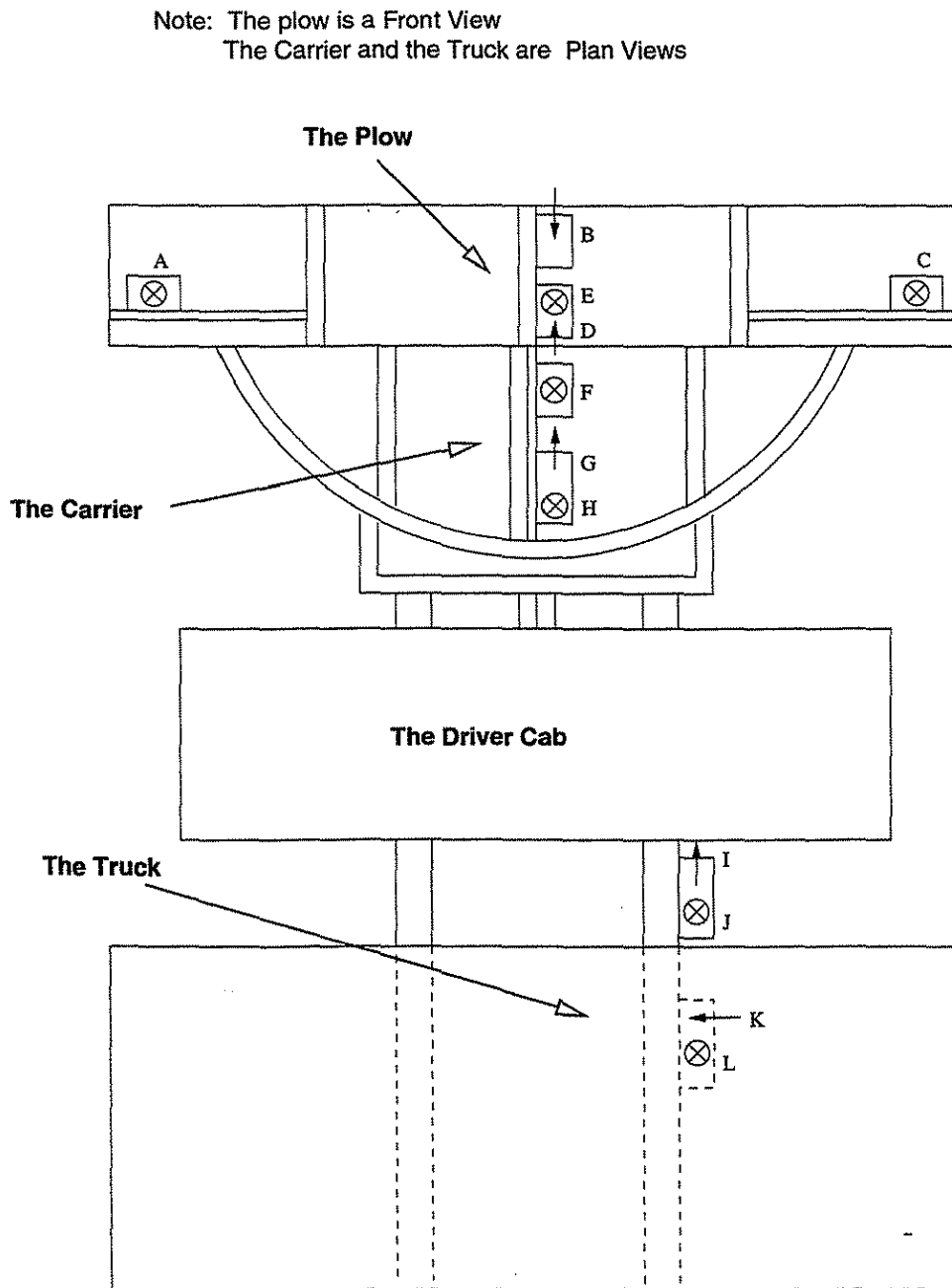


Figure 7. The placement of the accelerometers for the truck, carrier, and plow

In Fig. 7, the accelerometers A, E, and C in the plow were used to measure the accelerations in the horizontal direction, and accelerometers B and D to measure the accelerations in the vertical direction. For the carrier, the accelerometers F and H were used to measure the vertical accelerations, and accelerometer G to measure the horizontal acceleration. To prevent the accelerometers from damage by harsh environmental and weather conditions, they were installed in the boxes that were attached to the required positions, as shown in Fig. 8. To reveal the arrangement of accelerometers inside the boxes, the accelerometers E, D and F presented in Fig. 7 are shown in Fig. 9. The cables connecting the accelerometers were linked to a Kistler power supply/coupler that was located at the passenger's side in the driver cab (see Fig. 10a). A Cyber Research 486 field computer (Fig. 10b) with Labtech Notebook data acquisition software was used to collect and display signals from the accelerometers. After finishing instrumentation and before winter time, the truck was driven to an abandoned pavement to run a few tests so that any problems in the instrumentation and data acquisition system could be found and modification could be made accordingly.

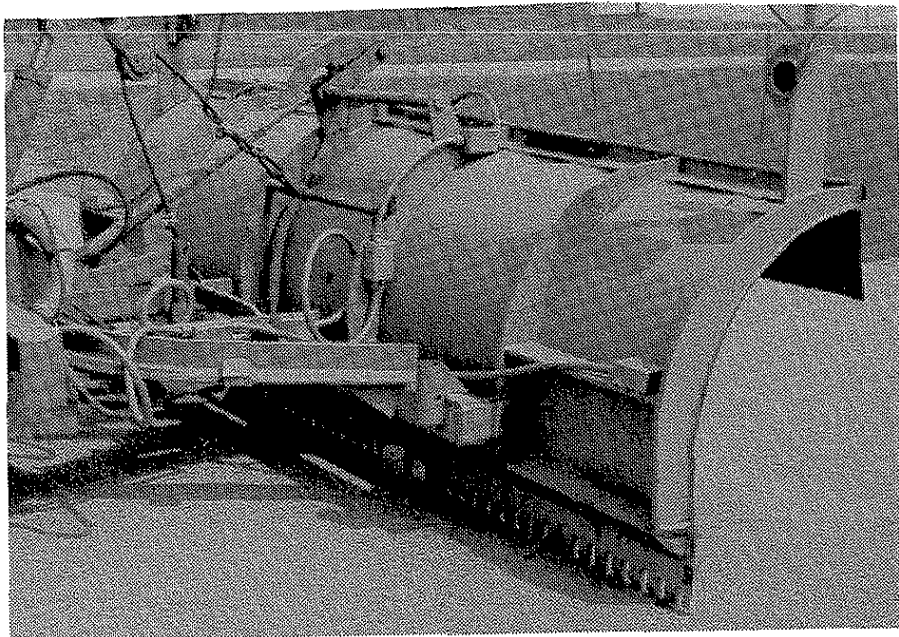


Figure. 8 Accelerometers are installed in the boxes attached to the plow and carrier

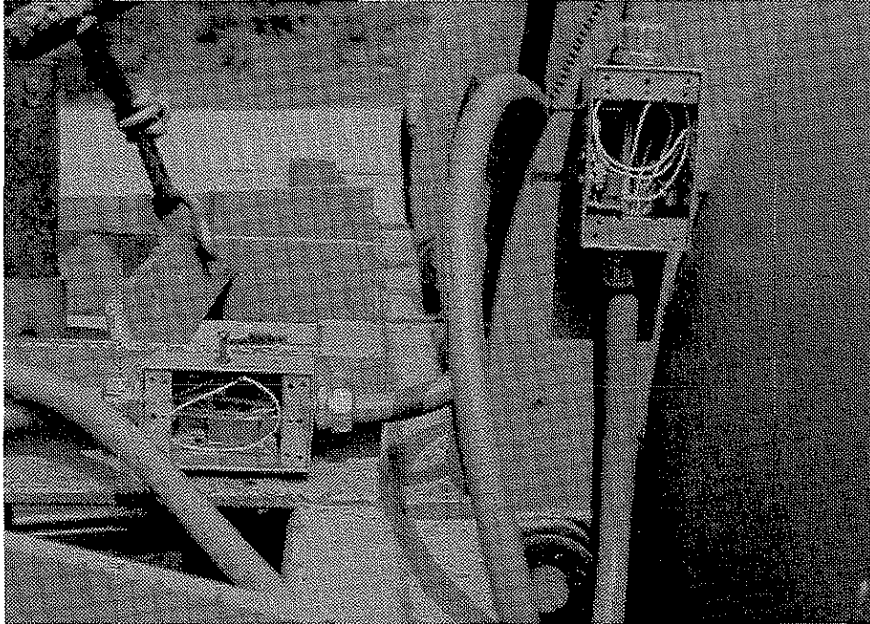


Figure 9. Details of the accelerometers inside the boxes

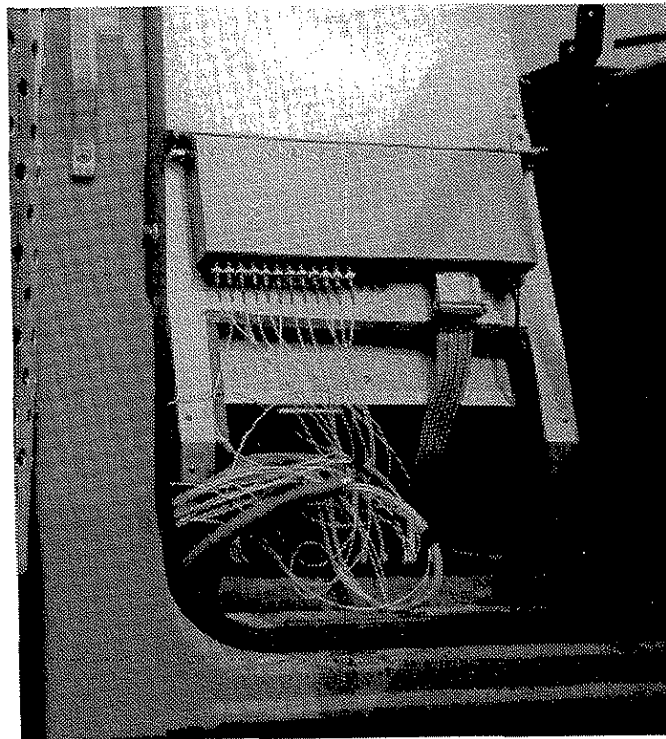


Figure 10. (a) The power supply/coupler for the accelerometers,

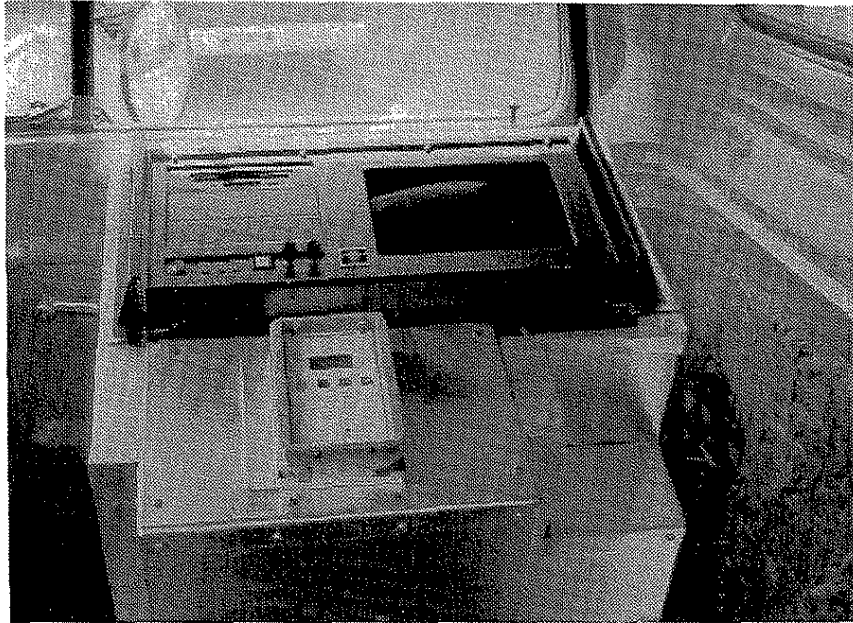


Figure 10. (b) The computer with data acquisition system

III. EXPERIMENTAL PROCEDURE

A. Preparation of Ice Sheet. The spillway apron of the Coralville Reservoir located about five miles north of Iowa City was chosen as the test site. The procedure to prepare ice sheets was the same as that used by Nixon and Frisbie (1993) in Project HR 334. Briefly, ice sheet preparations were conducted at night under favorable weather conditions when overnight low temperatures were no more than -7°C . A 2850 liter (750 gallon) water tank in a truck was filled with chilled water (about 2°C). A 3hp pump at the back of the tank delivered the water at 41kPa (60 psi) to a spray nozzle to spray the water uniformly over the pavement with a 7.5m wide spread. By driving the truck back and forth over the testing area at speeds about 0.6m/sec, an ice sheet of 54 meter long and 7.5 meter wide was formed. The ice sheet was then left to harden overnight and the test would take place the following morning. The thickness of the ice sheets so formed varied from 5mm to 10mm.

B. Scraping procedure. The measurement of accelerations requires that the truck begin its motion from a still stage. Therefore, the truck was positioned at one end of

the ice sheet with front plow sitting on the ice, and scraping operation was then started by driving the truck onto the ice sheet. At the same time, the data acquisition program was triggered to begin data collection. The truck was gradually accelerated to reach and keep at a velocity of 10 mph.

To provide better traction of the tires during scraping the truck was fully filled with gravel. Before testing the ambient temperature, the ice thickness, and ice conditions were recorded. The scraping procedures were videotaped to provide a visual record.

IV. RESULTS AND PROBLEMS

Preliminary field tests were conducted during the 1995-1996 winter season, using an "as is" truck with a front mounted plow provided by Iowa DOT. It was found that no ice was removed by the plow although it was a heave type plow. The plow was not able to cut into the ice, but skipped and slipped over the ice surface. The cutting edge on the plow was a standard cutting edge. While these tests were not successful at scraping ice, they did allow development of the instrumentation.

During the 1996-1997 winter, six field tests were performed using the same truck instrumented with accelerometers and data acquisition system. The testing temperatures (ambient temperatures) were about -6 to -10°C. This time serrated cutting edges were used instead of standard ones. Unfortunately, the results were again disappointed: the plow was found not able to remove the ice except that some teeth of the cutting edge occasionally chipped off a few ice fragments.

It should be noted that as many different configurations as possible for the front plow were tested. However, no permanent alterations to the plow or hitch were made.

Another problem experienced in the field tests was that the truck tended to lose traction at speeds higher than 10mph. There were some occasions during which the truck was out of control and span over the ice surface, creating a dangerous situation. This might be an indication that the current front-mounted plows seem not to be favorable equipment for ice removal unless some fundamental improvement of these plows is achieved. This point is discussed further below.

While the field tests showed negative results in terms of ice removal, it is still interesting to have a look at the data collected by the accelerometers and the data acquisition system. Fig. 11 presents the plots of the accelerations measured by the accelerometers mounted on the plow and the carrier. The plots in Figs 11a, c, and e show the horizontal accelerations at three different points on the plow as measured by accelerometers A, C, and E (see Fig. 7), and the plots in Figs 11b and d represent the vertical accelerations of the plow as measured by accelerometers b and d. The horizontal acceleration of the carrier is illustrated by the plot in Fig. 11g and the vertical accelerations by Figs 11f and h, as measured by accelerometer G and accelerometers F and H, respectively.

A major feature illustrated by the plots in Fig. 11 is that the signals are fluctuating rapidly and violently, indicating that the response of the plow and the carrier when scraping ice was indeed very much a dynamic one. However, since the plow essentially cut no ice, these signals were not caused by the cutting forces, but caused mainly by the vibration of the plow and carrier. Those peak values shown in each plot are believed to correspond to the forces experienced by the plow and carrier when some teeth of the cutting edge occasionally chipped the ice. There is a maximum value in each plot occurring close to the 6 second point on the abscissa, which in fact corresponds to the event when the plow hit a concrete joint. It is also evident from the plots that these signals are fluctuating more or less symmetrically with respect to the zero value. This again is an indication that the plow and carrier were vibrating and skipping over the ice surface. These signals are excellent for analyzing the characteristics of vibration of the plow, but are less meaningful for determining the scraping forces.

Another attempt to analyze the acquired data was made by performing Fast Fourier Transforms (FFT). FFT is a powerful tool for spectral analysis of dynamics problems, which allows the data to be examined in frequency domain. A useful outcome of FFT is the Power Spectrum through which the magnitude of a sampled waveform can be estimated. The definition of the Fourier transform of a signal $x(t)$ is

$$X(f) = F(x\{t\}) = \int_{-\infty}^{\infty} x(t)e^{-j2\pi ft} dt .$$

However, the actual output of FFT of the collected data is given by the following equation

$$X_k = \sum_{i=0}^{n-1} x_i e^{-j2\pi k i/n} \quad \text{for } k = 0, 1, 2, \dots, n-1.$$

The power spectrum of the input signal is defined as

$$S_{xx}(f) = |X(f)|^2$$

The results of FFT for the data presented in Fig. 11 are shown in Fig. 12. The plots in Fig. 12 a, b, c, d, e, f, g, and h represent the power spectra of the data plotted in Fig. 11a, b, c, d, e, f, g, and h, respectively. It was expected that power spectral analysis would provide some useful information of the accelerations of the plow and carrier. However, as shown in Fig. 12, it is difficult to distinguish dominant spectrums in the frequency bands. One explanation for this is that random vibration of the plow and carrier was responsible for the signals collected. This is again indicative of the skipping phenomenon of the front plow over ice.

V. SUMMARY

This study explores the possibility of using accelerometers to determine the forces on a front-mounted plow when scraping ice. The plow was modeled by using a dynamic approach. The forces on the plow were to be determined by the measurement of the accelerations of the plow. Field tests were conducted using an “as is” front-mounted plow instrumented with accelerometers. The results of the field tests indicate that in terms of ice removal, the front-mounted plow is not favorable equipment in its configuration. However, the use of accelerometers seems to be promising for analyzing the vibration problems of the front-mounted plow. Additionally, it may be of value to investigate other methods of mounting front plows that allow down loads to be developed.

REFERENCES

Wilfrid A. Nixon and Todd R. Frisbie, 1993. "Field Measurements of Plow Loads during Ice Removal Operations", Final Report, Iowa Department of Transportation Project HR 334.

Scraping Test No. 3 (Ch. 1)

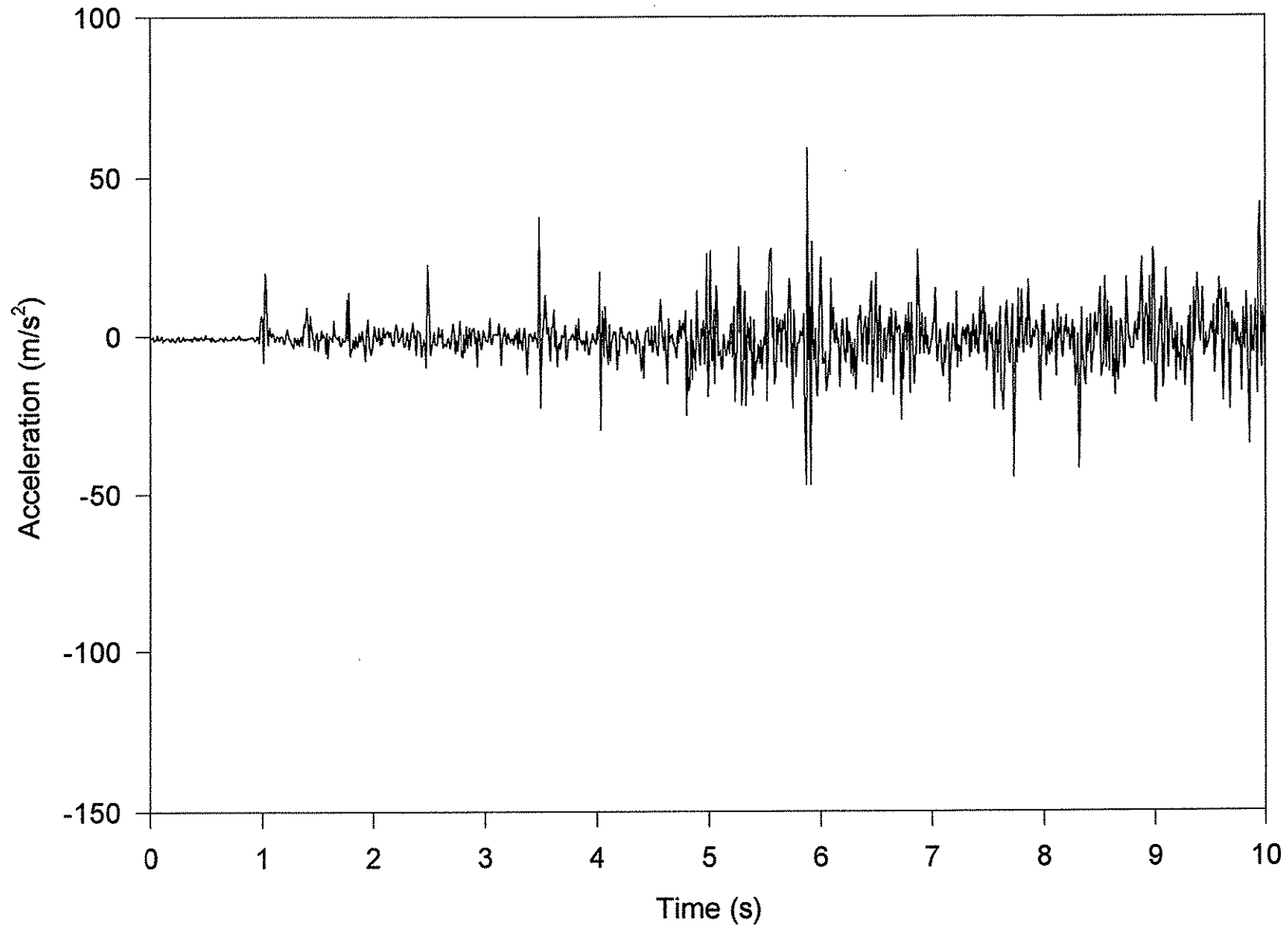


Figure 11 (a). The acceleration in x-direction measured by accelerometer A on the plow (Test No.3)

Scraping Test No. 3 (Ch. 2)

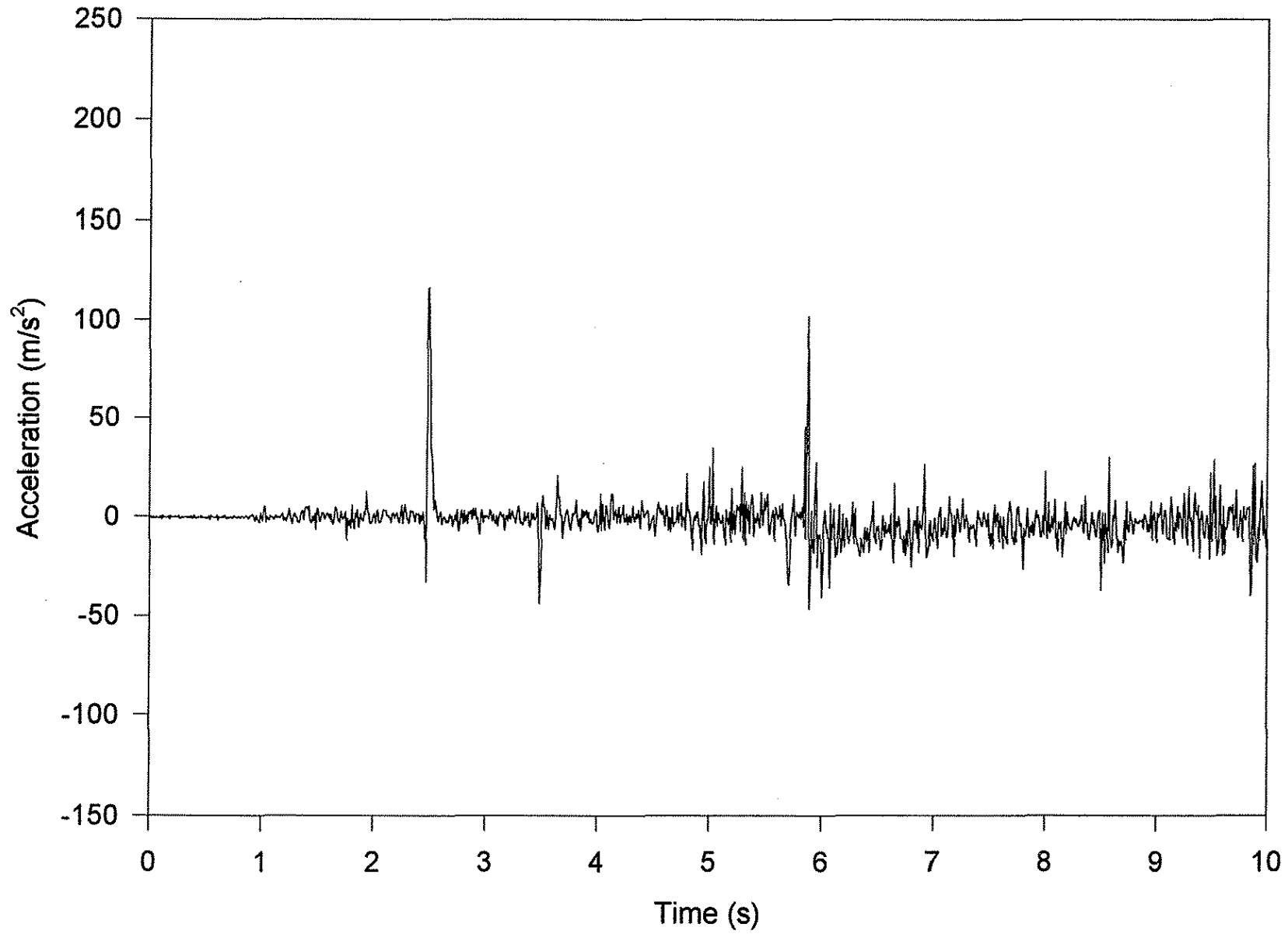


Figure 11 (b). The acceleration in y-direction measured by accelerometer B on the plow (Test No.3)

Scraping Test No. 3 (Ch. 3)

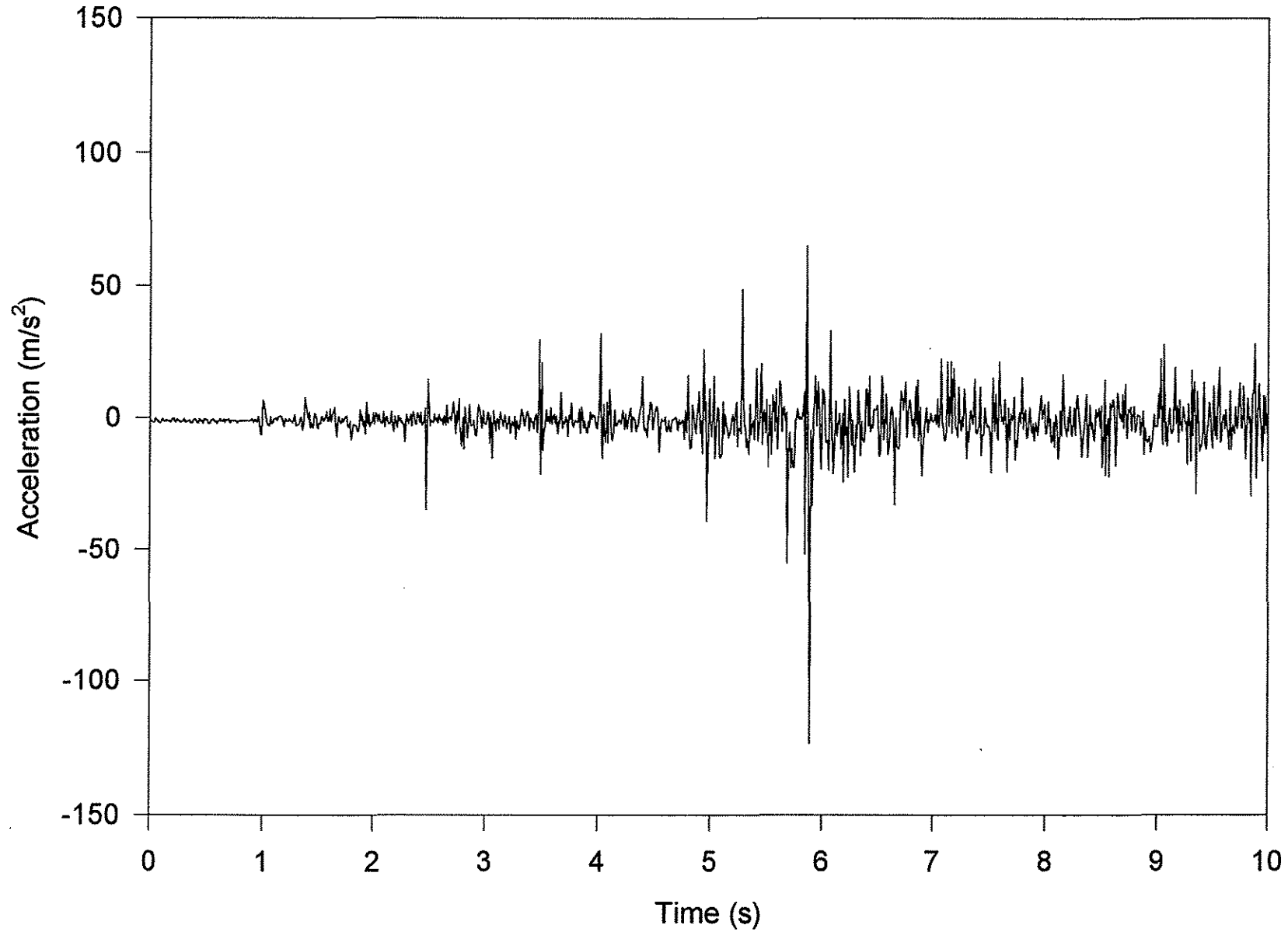


Figure 11 (c). The acceleration in x-direction measured by accelerometer C on the plow (Test No.3)

Scraping Test No. 3 (Ch. 4)

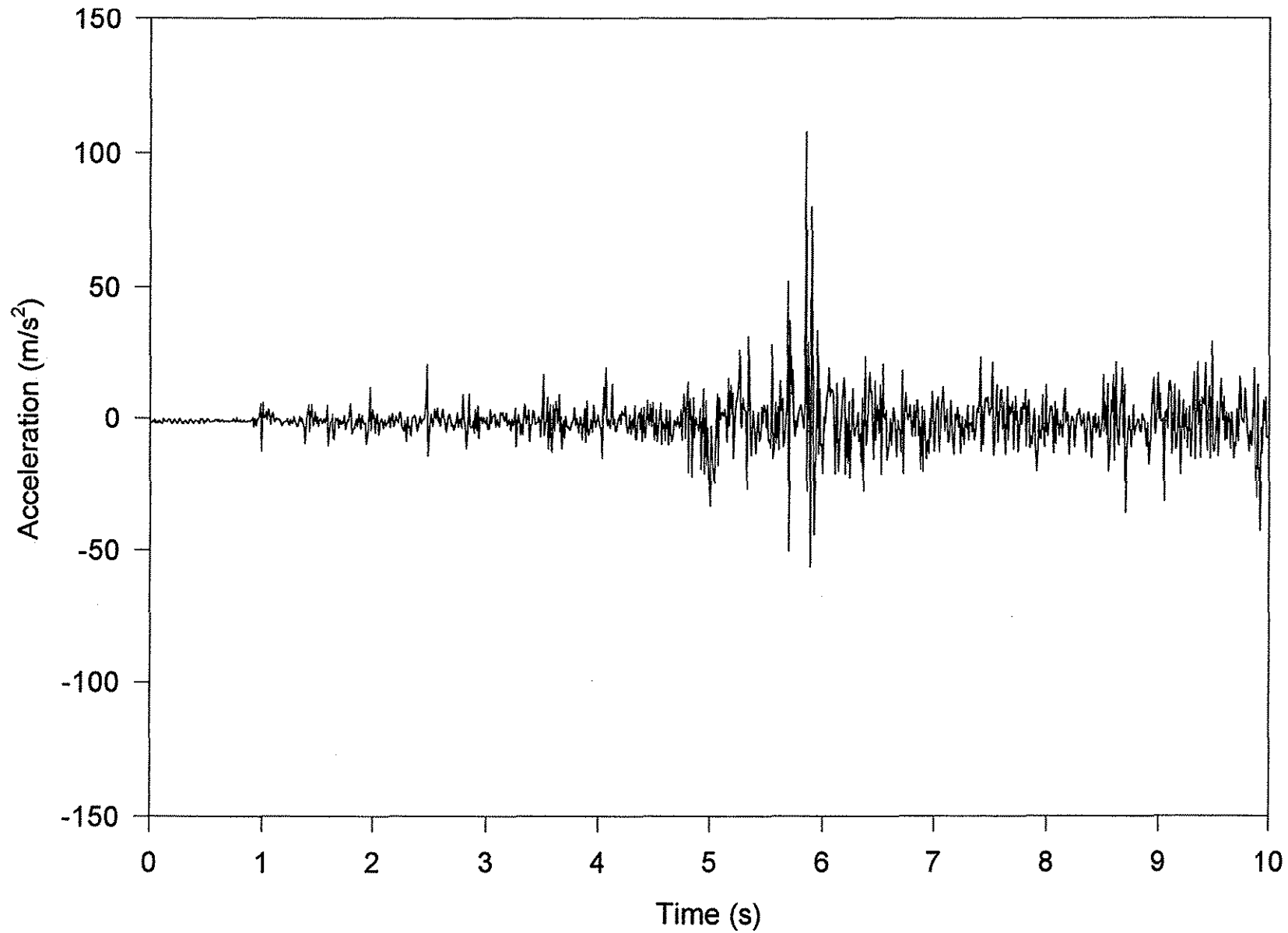


Figure 11 (d). The acceleration in y-direction measured by accelrometer D on the plow (Test No.3)

Scraping Test No. 3 (Ch. 5)

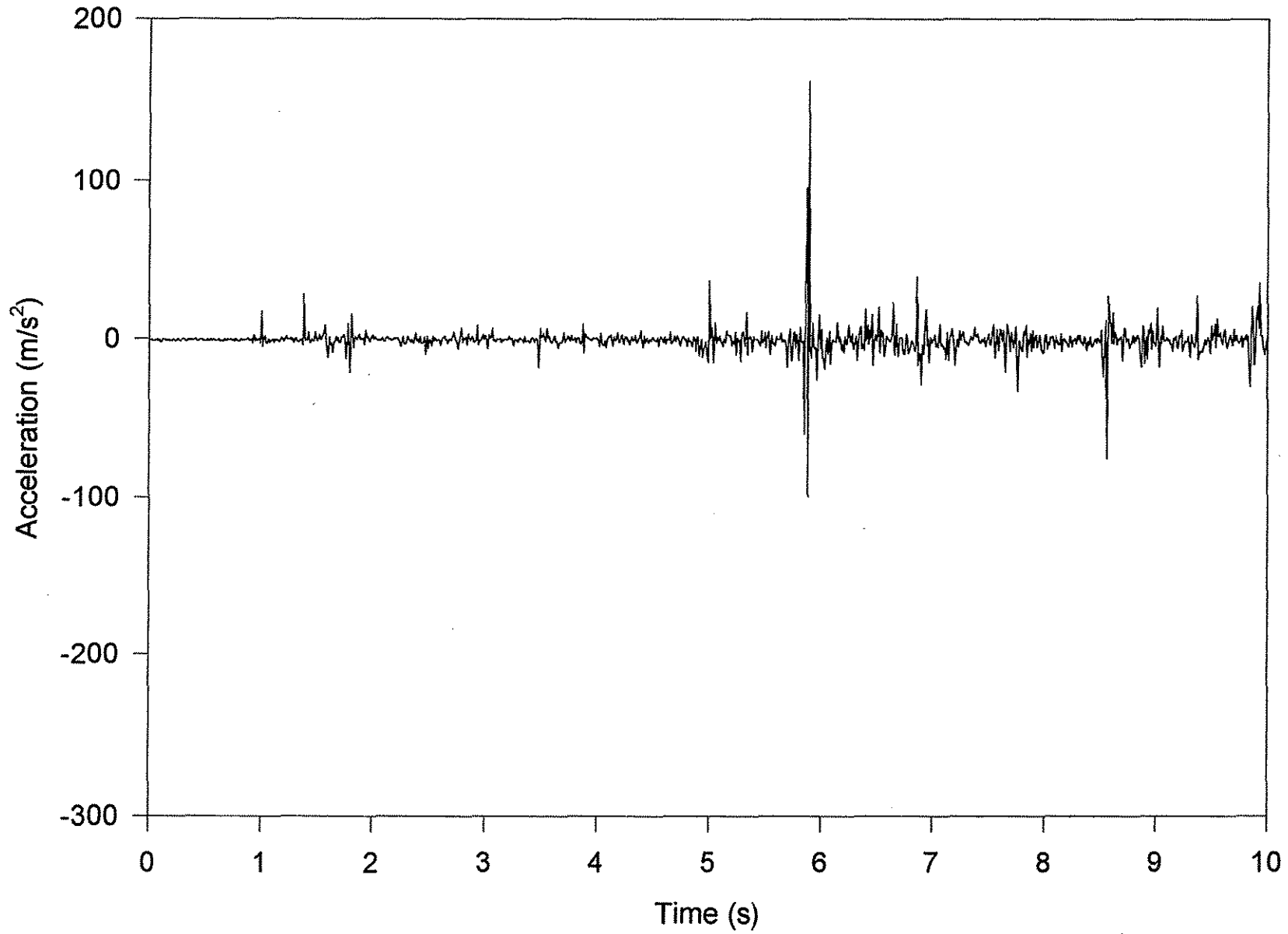


Figure 11 (e). The acceleration in x-direction measured by accelrometer E on the plow (Test No.3)

Scraping Test No. 3 (Ch. 6)

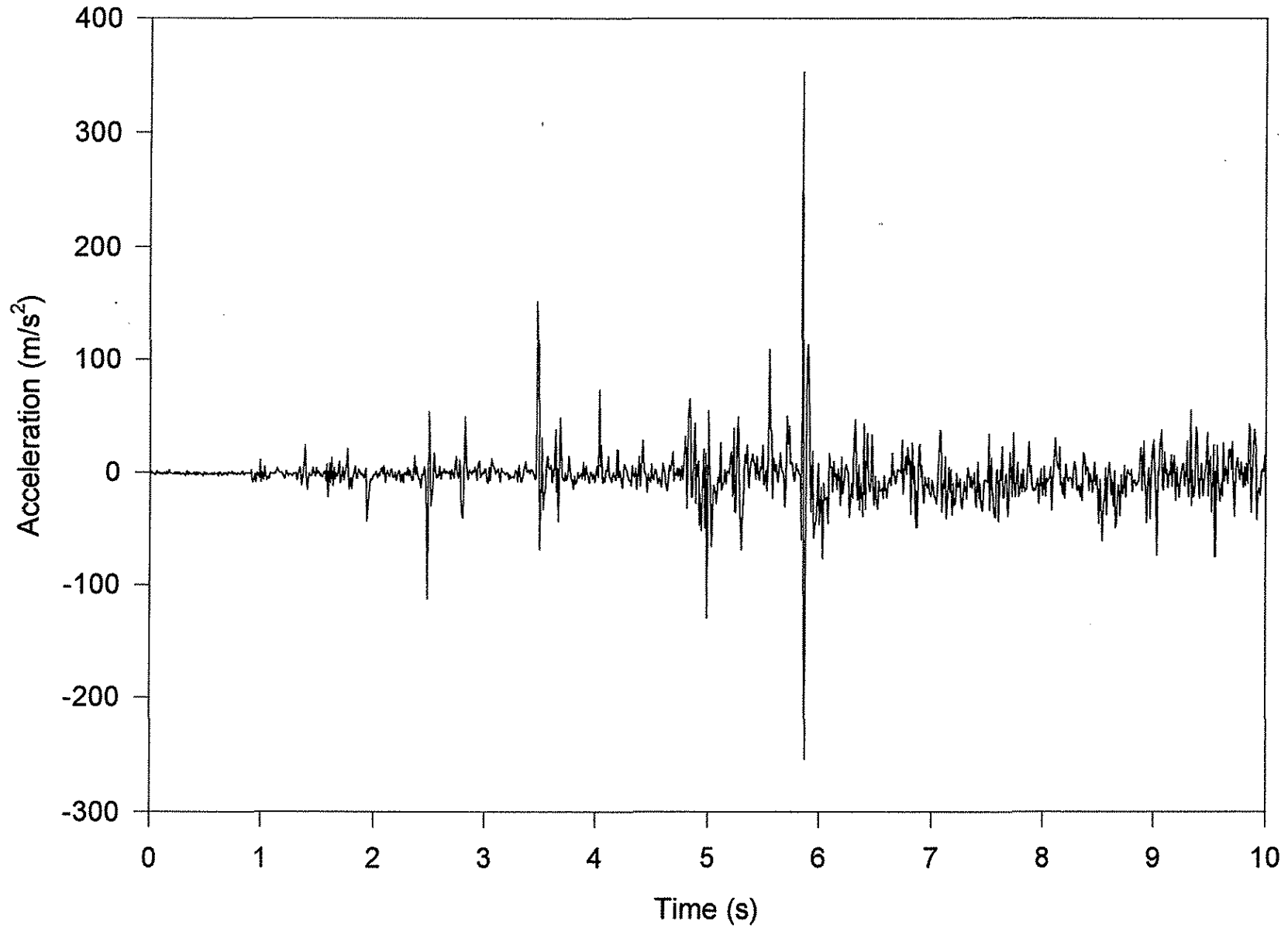


Figure 11 (f). The acceleration in y-direction measured by accelrometer F on the carrier (Test No.3)

Scraping Test No. 3 (Ch. 7)

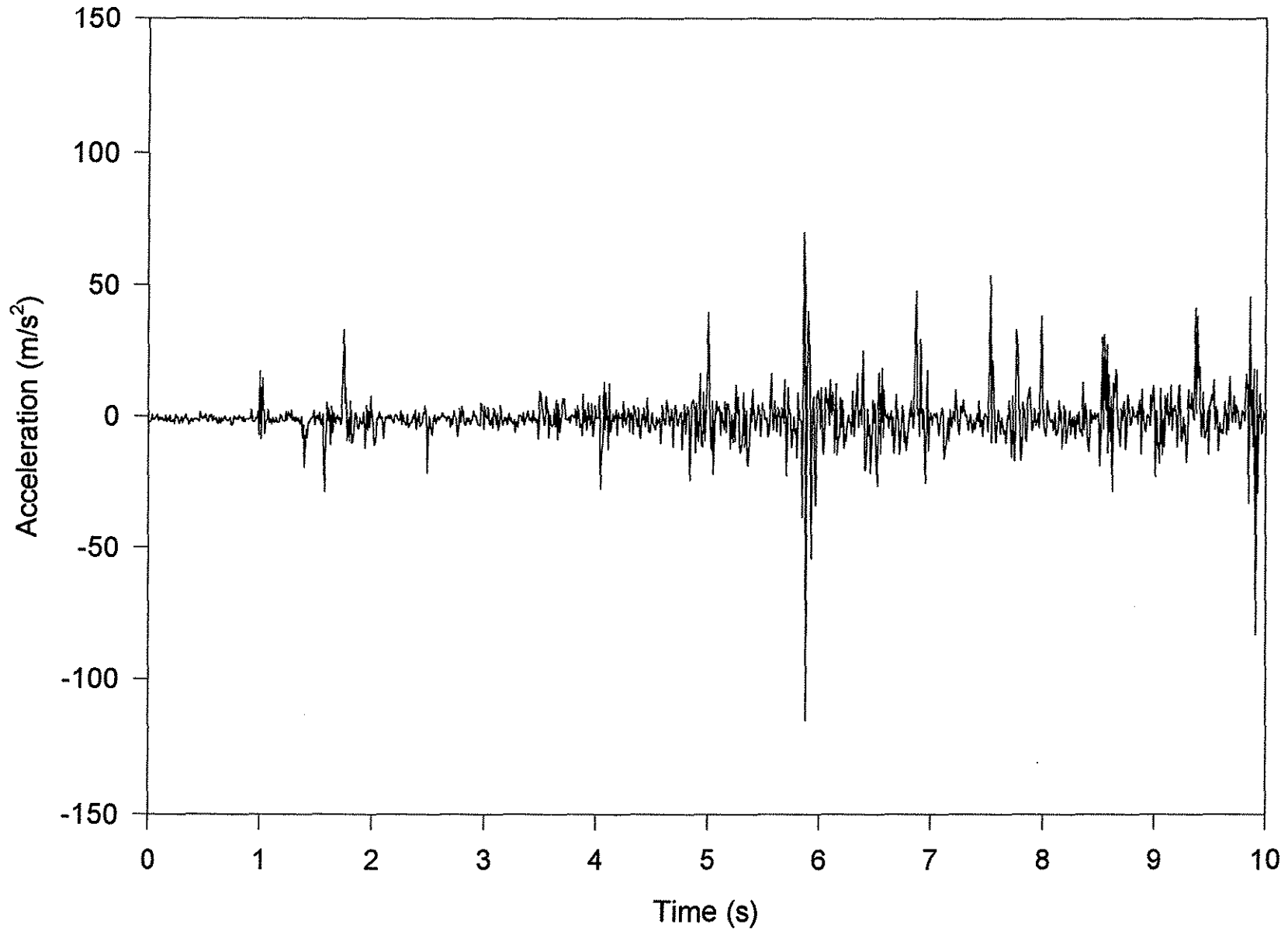


Figure 11 (g). The acceleration in x-direction measured by accelrometer G on the carrier (Test No.3)

Scraping Test No. 3 (Ch. 8)

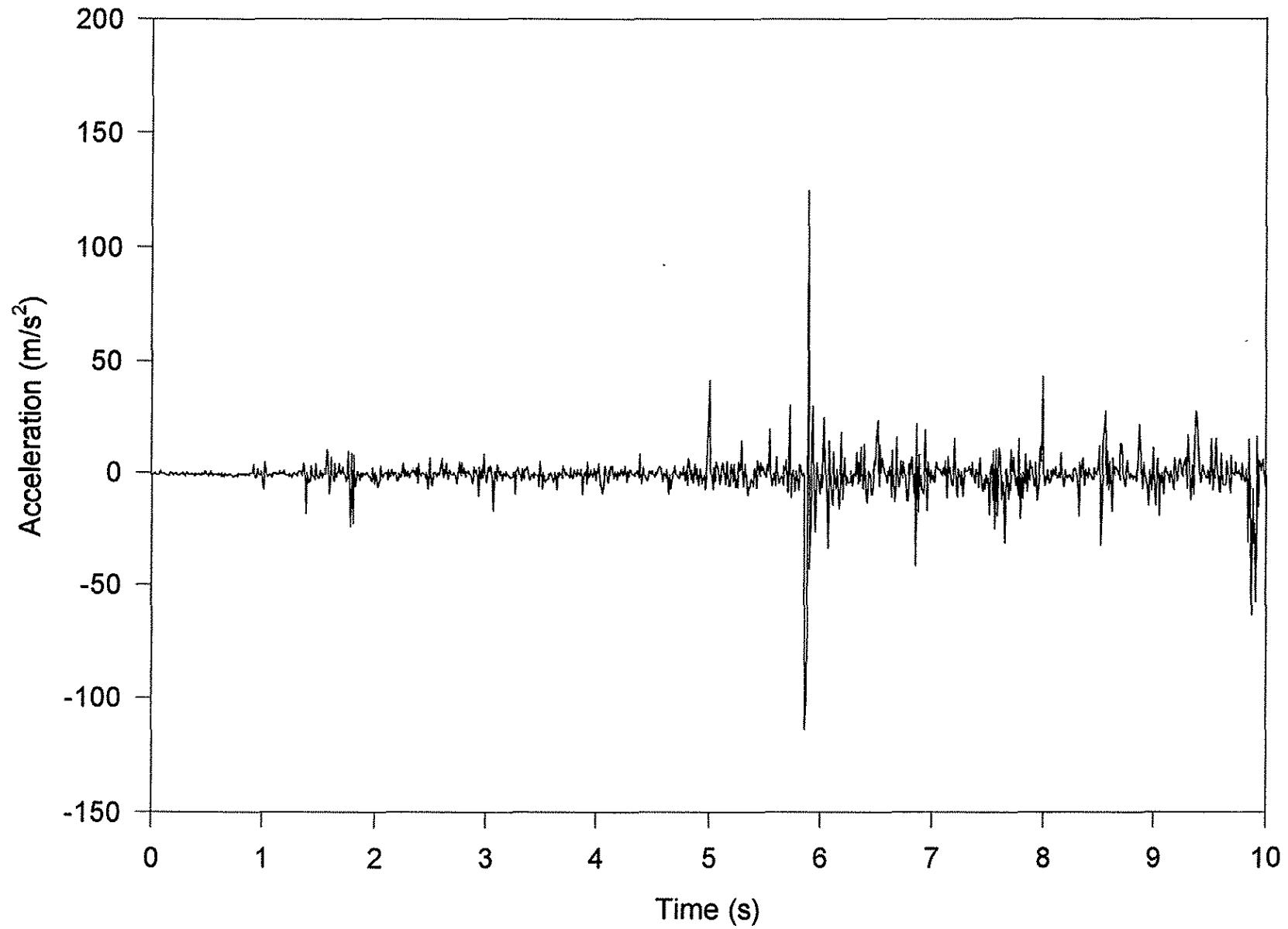


Figure 11 (h). The acceleration in y-direction measured by accelrometer H on the carrier (Test No.3)

FFT for Test No. 3 (Channel 1)

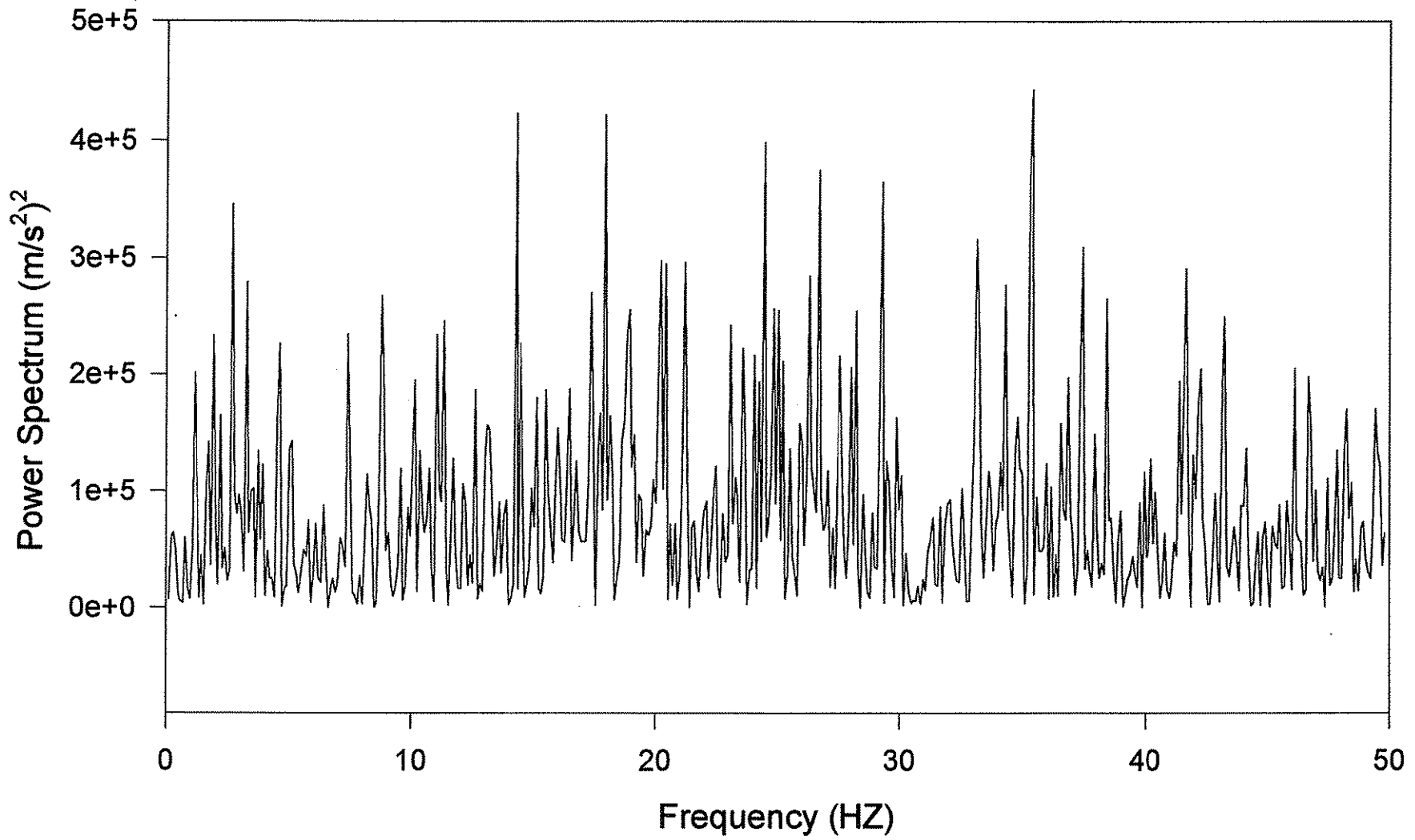


Figure 12. (a) The power spectrum of the signal from accelerometer A (Test No. 3)

FFT for Test No. 3 (Channel 2)

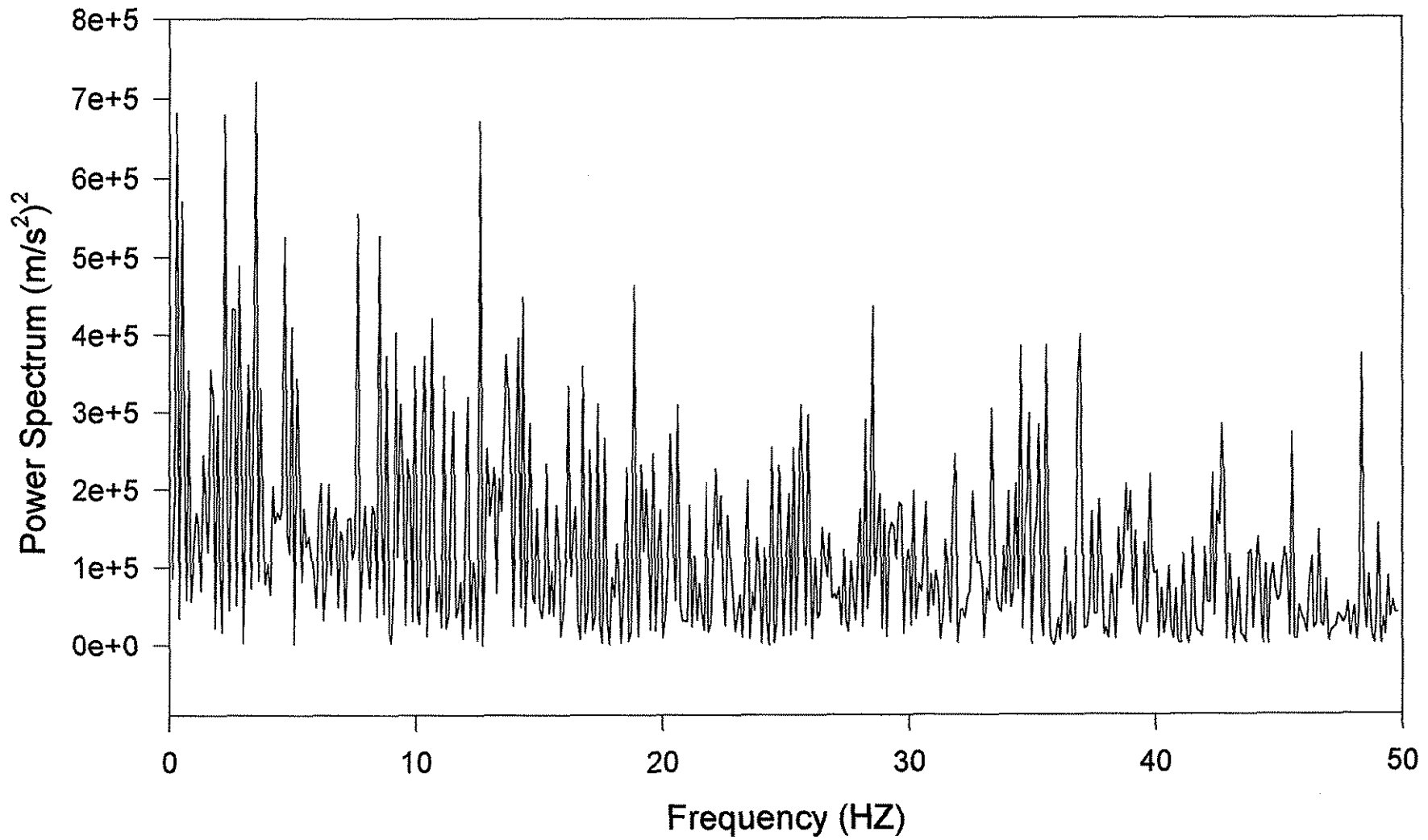


Figure 12. (b) The power spectrum of the signal from accelerometer B (Test No. 3)

FFT for Test No. 3 (Channel 3)

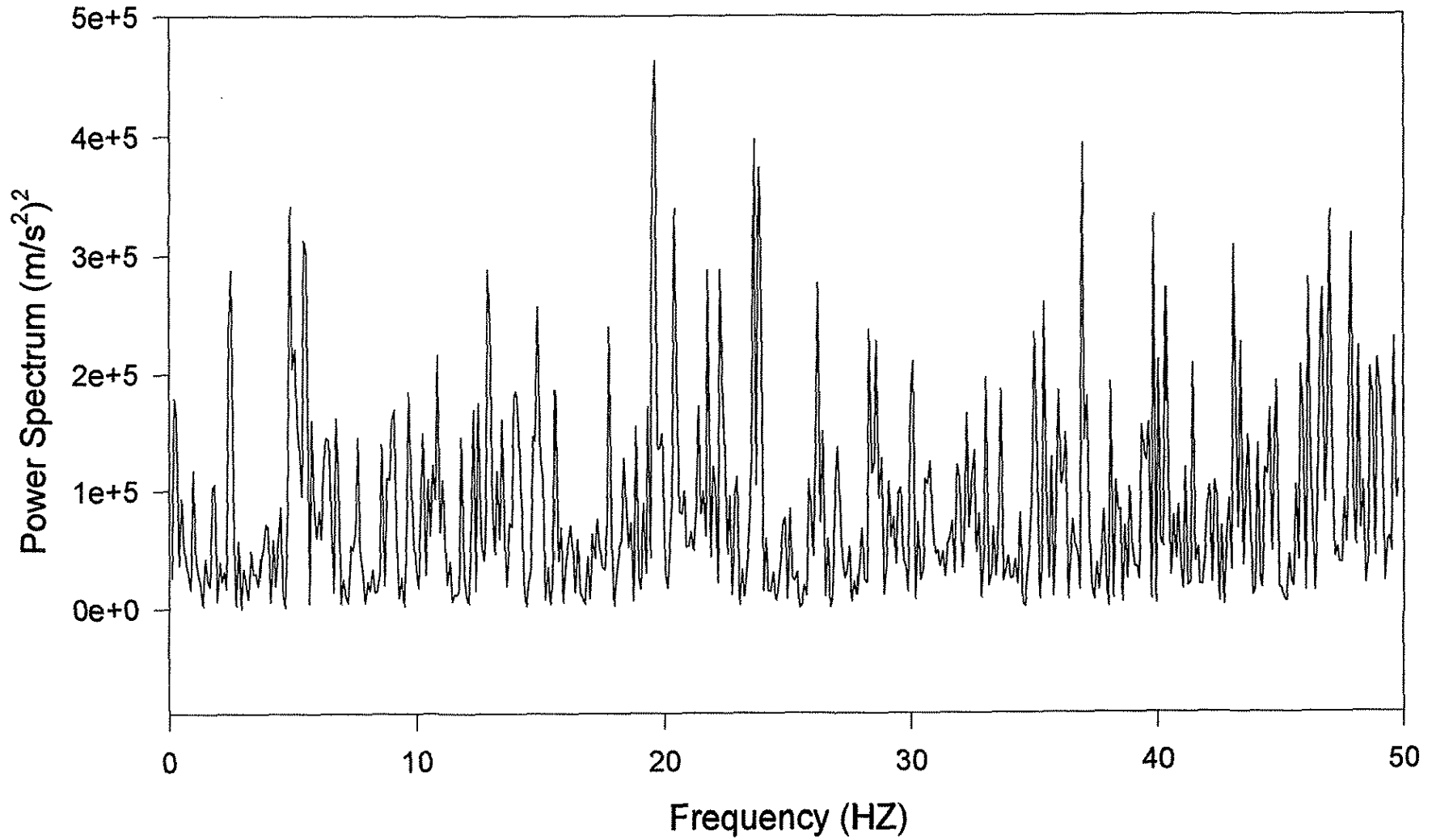


Figure 12. (c) The power spectrum of the signal from accelerometer C (Test No. 3)

FFT for Test No. 3 (Channel 4)

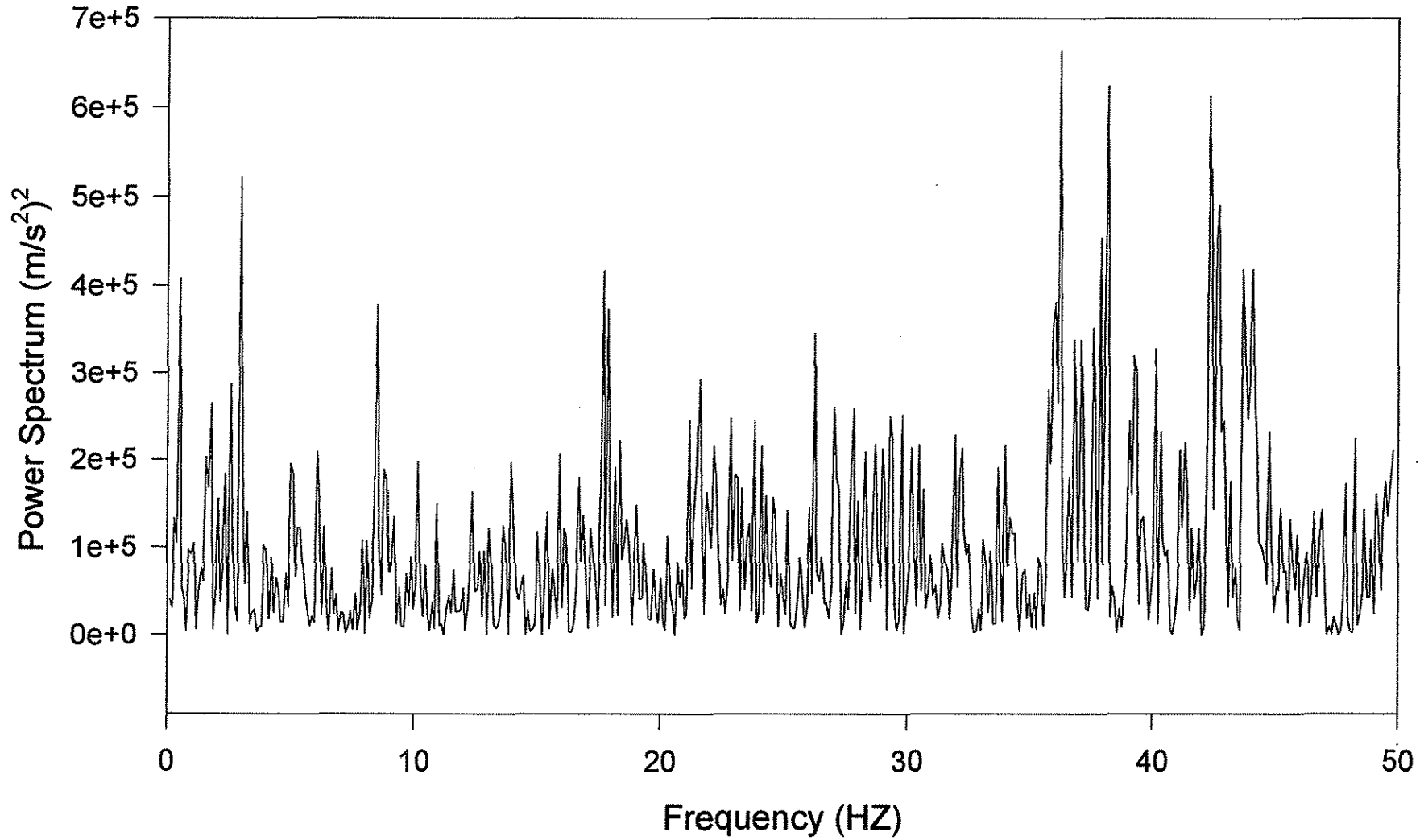


Figure 12. (d) The power spectrum of the signal from accelerometer D (Test No. 3)

FFT for Test No. 3 (Channel 5)

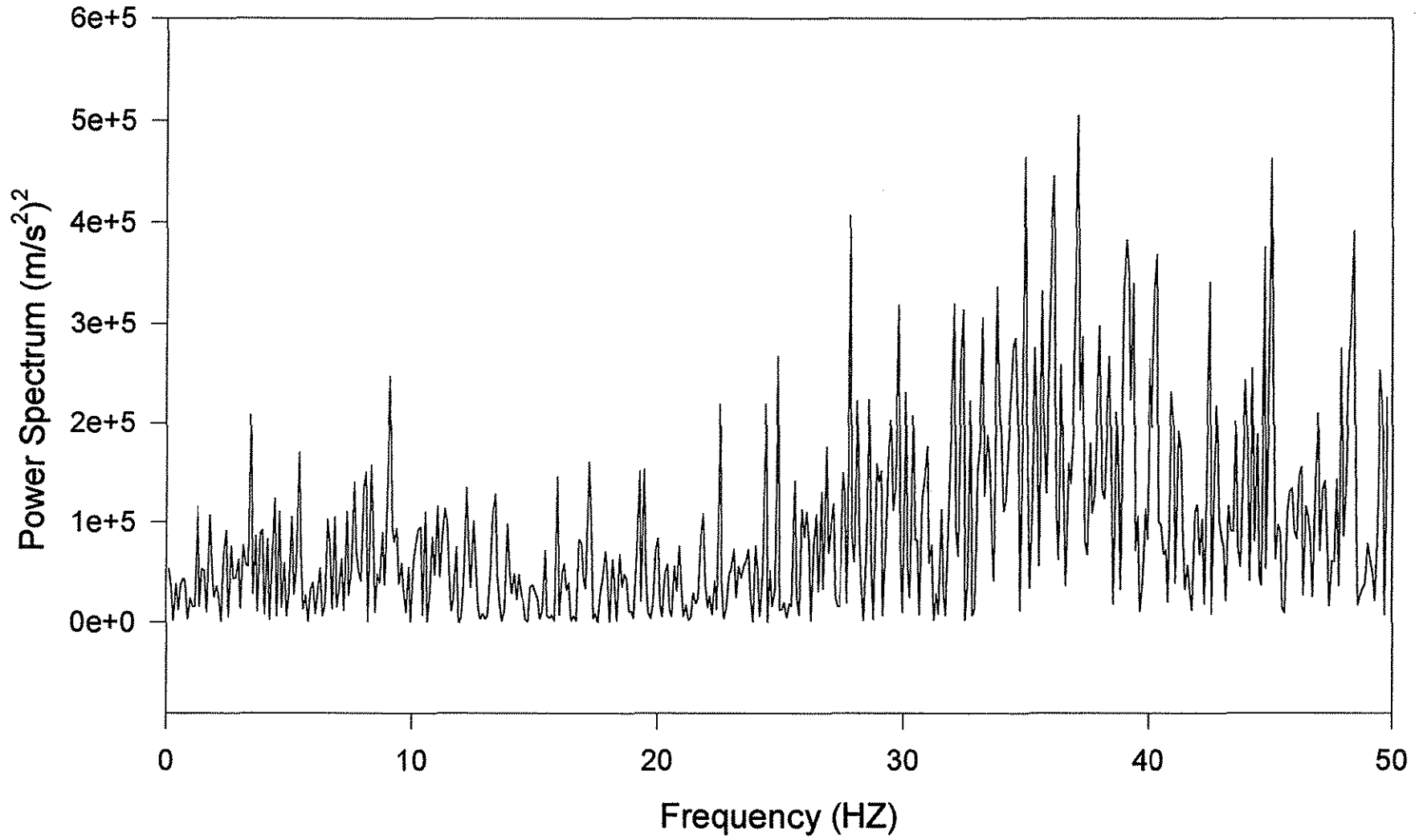


Figure 12. (e) The power spectrum of the signal from accelerometer E (Test No. 3)

FFT for Test No. 3 (Channel 6)

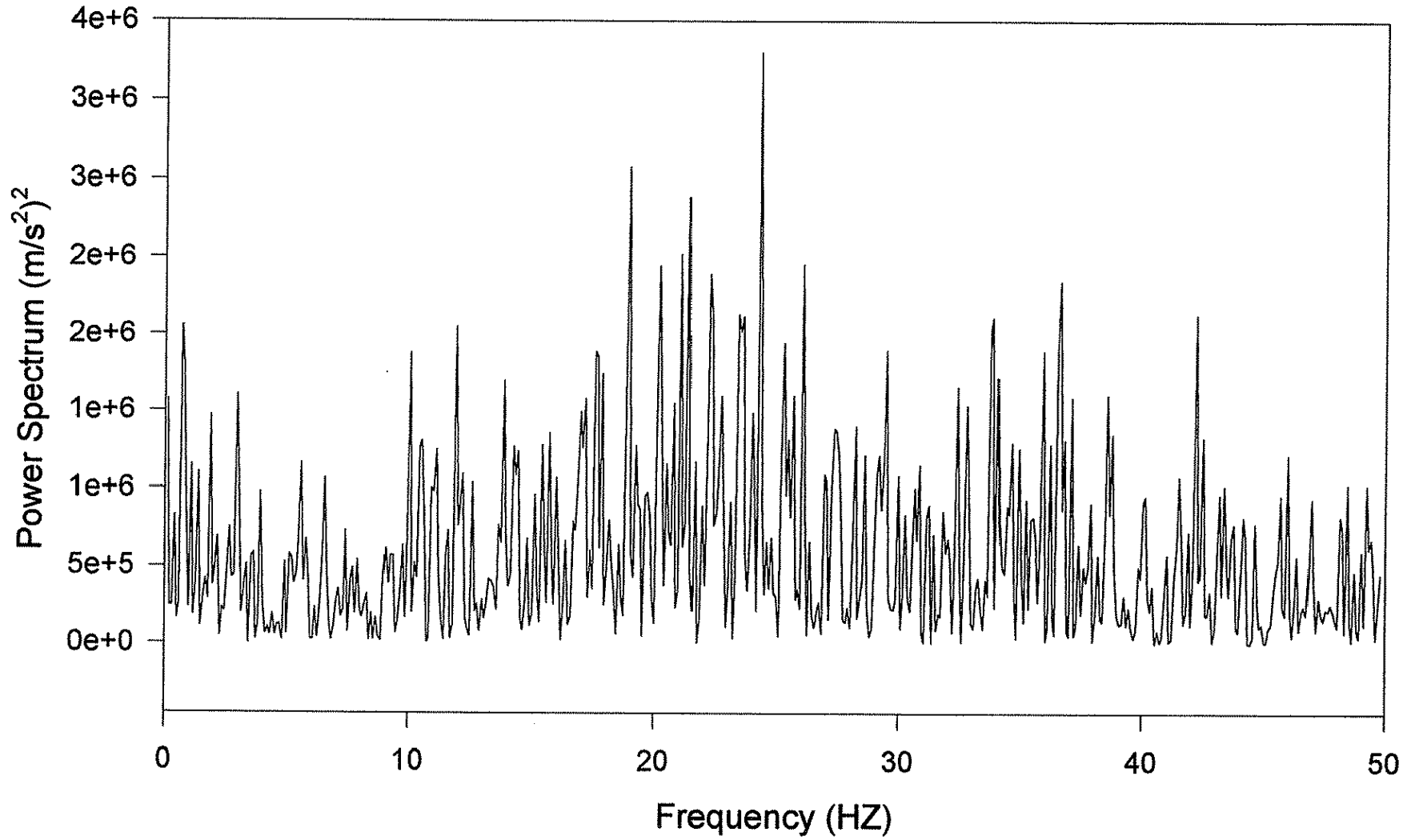


Figure 12. (f) The power spectrum of the signal from accelerometer F (Test No. 3)

FFT for Test No. 3 (Channel 7)

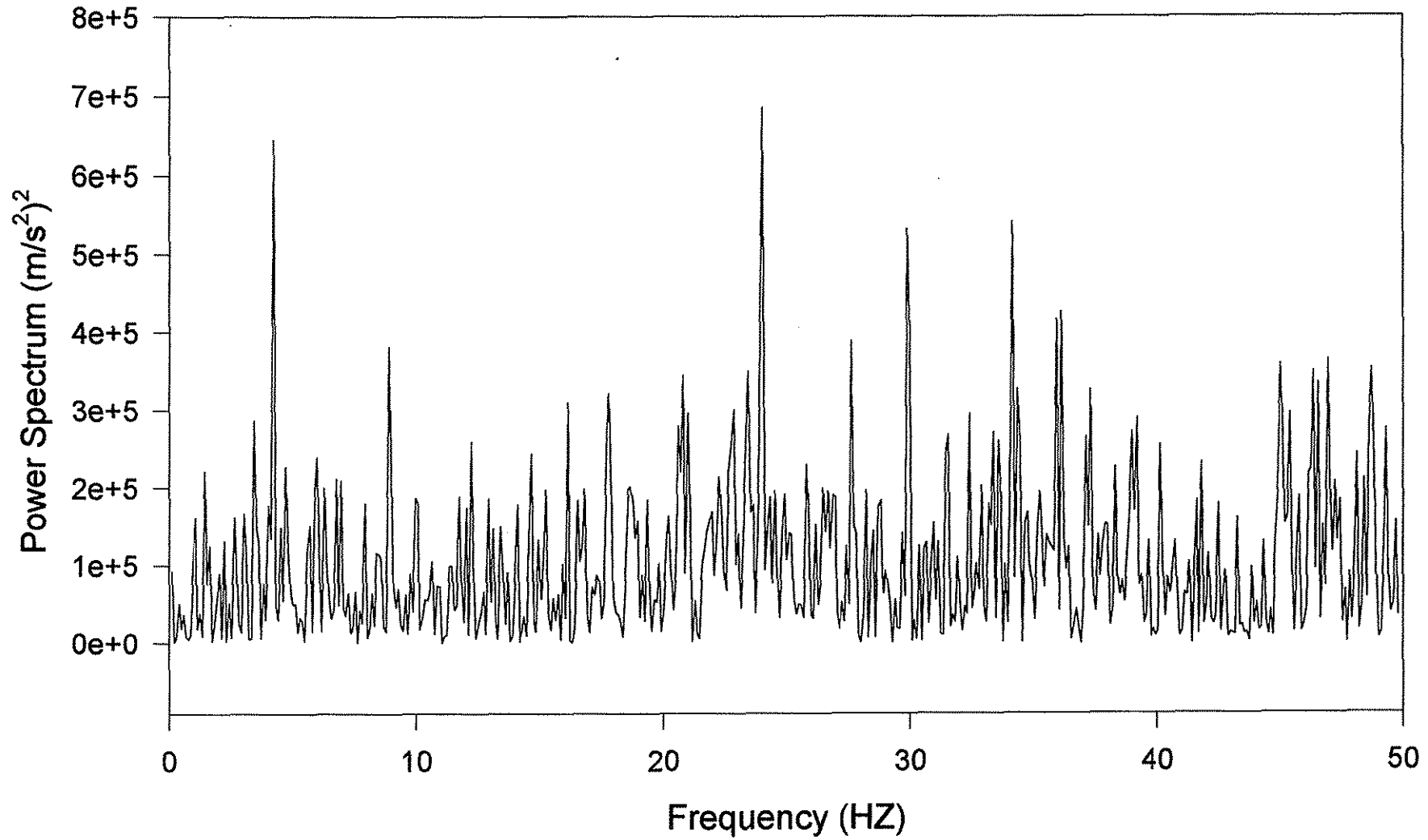


Figure 12. (g) The power spectrum of the signal from accelerometer G (Test No. 3)

FFT for Test No. 3 (Channel 8)

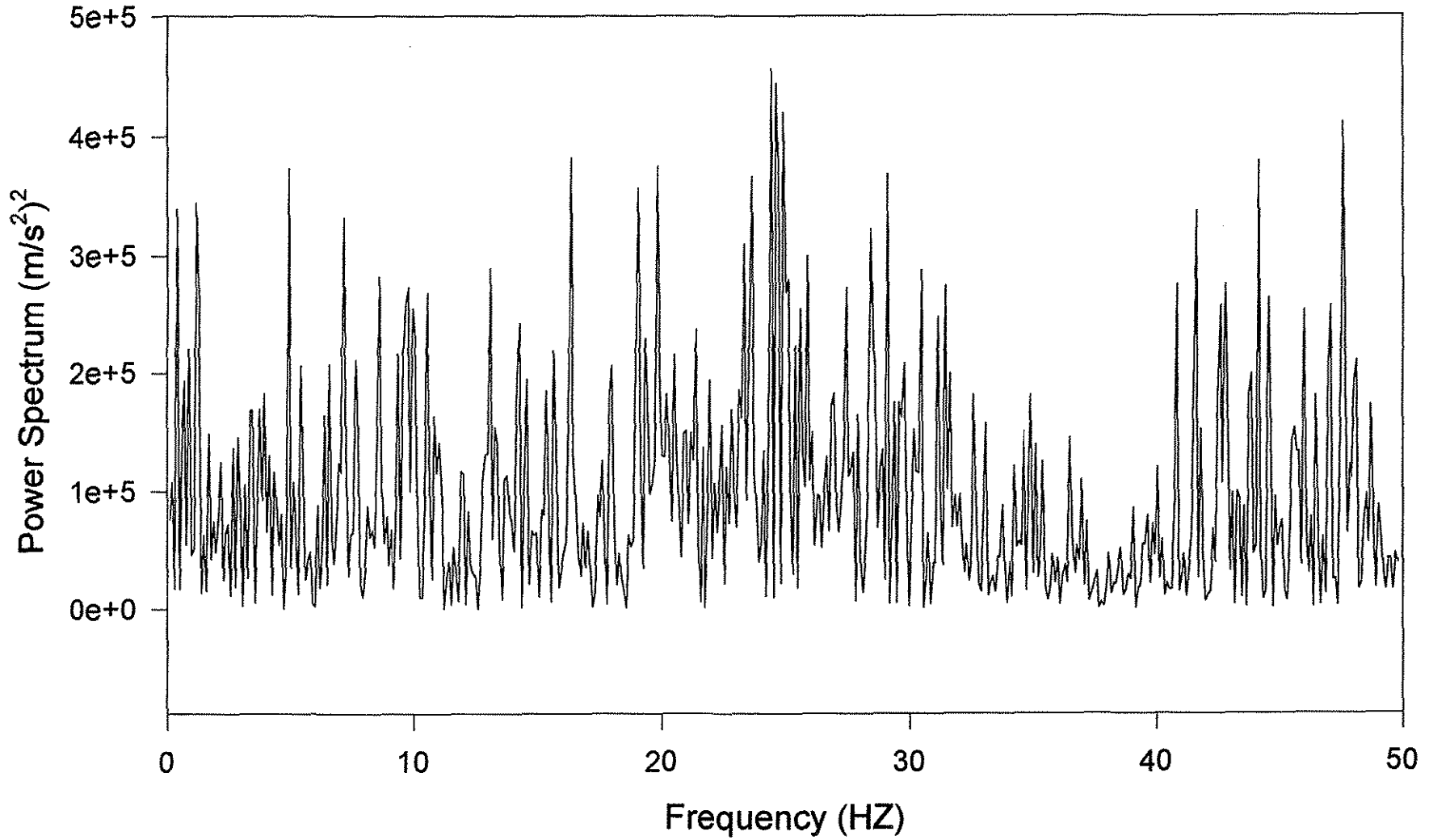


Figure 12. (h) The power spectrum of the signal from accelerometer H (Test No. 3)